http://dx.doi.org/10.5012/bkcs.2014.35.7.1933

Articles

An Image Cytometric MTT Assay as an Alternative Assessment Method of Nanoparticle Cytotoxicity

Song Hee Lee, Jonghoon Park, Dongwook Kwon, and Tae Hyun Yoon*

Department of Chemistry, Research Institute for Natural Sciences, Hanyang University, Seoul 133-791, Korea
**E-mail: thyoon@gmail.com*
Received October 14, 2013, Accepted December 22, 2013

Despite increasing importance of *in vitro* cell-based assays for the assessment of nanoparticles (NPs) cytotoxicity, their suitability for the assessment of NPs toxicity is still in doubt. Here, limitations of widely used cell viability assay protocol (*i.e.*, MTT asssay) for the cytotoxicity assessment of P25 TiO_2 NPs were carefully examined and an alternative toxicity assessment method to overcome these limitations was proposed, where the artifacts caused by extracellularly formed formazan and light scattered by agglomerated NPs were minimized by measuring only the intracellular formazan *via* image cytometric methods.

Key Words : Alternative assay method, Nanoparticles cytotoxicity, Image cytometry, MTT assay, TiO_2 nanoparticles

Introduction

Due to increasing concerns on the potential hazards of manufactured nanomaterials, a large number of studies have been reported on the cytotoxicity of nanoparticles (NPs).[1,2] However, reports on the limitations and challenges related to assessing NPs toxicity are also accumulating in the literature, [3-9] which is partially attributable to the inability of current cytotoxicity assay protocols to quantitatively assess biological responses related to NPs toxicity.[2,4-7,10] For instance, various cell viability assays, such as the mitochondrial reduction of MTT (3-(4,5-Dimethyl-2-thiazolyl)-2,5-diphenyl-2*H*-tetrazolium bromide) to formazan, have been recently tested for their suitability in assessing nanotoxicity.[5-8] According to these studies, NPs interacting with indicator dyes (*e.g.*, *via* adsorption, catalytic reaction, or optical interferences) might result in errors during many *in vitro* nanotoxicity assays.[3] Moreover, certain NPs, such as SWCNT[7] and PSi[5] interact with MTT to induce significant artifacts in cell viability assays. Therefore, developing alternative assay protocols that can reliably and accurately assess NPs cytotoxicity is crucial for the unbiased assessments of NPs cytotoxicity and has utmost importance in providing solid scientific basis for future regulation of manufactured nanomaterials. In this study, to achieve these goals, we carefully examined potential artifacts of the conventional MTT cell viability assay protocol in assessing the cytotoxicity of P25 TiO_2 NPs. Based on these findings, we also developed an alternative approach based on image cytometry, which minimized artifacts caused by extracellular formazan formation *via* measuring only the intracellular formazan.

Experimental

Preparation of TiO_2 NPs. The aeroxide P25 TiO_2 used in this study was provided by the manufacturer (lot no. 4168112198, Evonik GmbH, Germany). Stock solutions of 10 g/L P25 TiO_2 powder were prepared by dispersing bulk powder in deionized water and sonicated for 10 min using a probe sonicator (420 W, 20 kHz, Sonosmasher, Ulsso Hitech, Korea). The sub-100 nm fractions of the TiO_2 suspension were prepared by centrifugation at 6,800 g for 20 min (mega 17R, Hanil Science Industrial, Korea), from which the supernatant was carefully removed.

Characterization of TiO_2 NPs. Recently, Kwon *et al.* in our group reported about dispersion, fractionation and characterization of sub-100 nm P25 TiO_2 nanoparticles in aqueous media. In this study, TiO_2 nanoparticles were used bulk and sub-100 nm sized P25 TiO_2 nanoparticles introduced in above article.[11]

The powder X-ray diffraction (XRD) pattern was measured using a Cu-Kα radiation source (D/max-2000, Rigaku, USA). The relative amounts of anatase and rutile phases were calculated from the integrated areas of the anatase (101) and the rutile (110) peaks, using Scherrer's equation. Analysis of the XRD pattern showed that the TiO_2^{P25} powder used in this study is composed of anatase (87%) and rutile (13%) crystalline phase. The mean sizes, estimated from the Scherrer line broadening analysis of the XRD data, were 19 nm for anatase and 54 nm for rutile. The surface area of powder TiO_2 dried at 90 ^oC for 5 h was determined by multipoint Brunauer Emmett Teller (BET) analysis with N_2 as the adsorbate on (nano-POROSITY, Mirae SI, Korea). The BET

specific surface area and the average particle diameter estimated from the BET surface area were 57 m^2/g and 30 nm, respectively. To measure the TiO_2 concentration, samples were digested with HNO_3 + HCl + HF and analyzed by using ICP-AES (Optima- 4300, Perkin Elmer DV, USA). The initial concentration of bulk TiO_2 suspension was 10,000 mg/L, but supernatant concentration after centrifugation at 6,800 g for 20 min was 142 mg/L.

The hydrodynamic size of nanoparticles in aqueous solution was examined using a dynamic light scattering (DLS) instrument (ScatteroscopeI, Qudix Inc, Korea). As results, mean hydrodynamic size of each TiO_2^{P25} fraction was measured as ~298 nm, and ~72 nm. The zeta potentials of TiO_2 dispersions were measured using a Zetasizer (Nano-ZS, Malvern instruments, UK). Representative image of TiO_2 nanoparticles and their aggregates were obtained by transmission electron microscopy (TEM) (H-7600, Hitachi, Japan).[11]

Nanoparticles Dispersion in Cell Culture Media. For the test of colloidal stability under cytotoxicity test media conditions, Dulbecco's Modified Eagle's medium (DMEM, Welgene, Daegu, Korea) were prepared with 0.001, 0.01, 0.1, 0.5, 1, 5 and 10% (v/v) of fetal bovine serum (FBS, Gibco, Grad Island, NY, USA), and mixed with TiO_2 supernatant solutions. Before mixing with other reagents, FBS was heated in 50 water bath and filtered through 0.20 μm sieve. The final concentration of TiO_2 was 14.2 mg/L and final FBS content was 0.0009, 0.009, 0.09, 0.45, 0.9, 4.5, 9% (v/v). TiO_2 nanoparticles are stabilized under DMEM cell culture medium condition including 0.09% of FBS.[12]

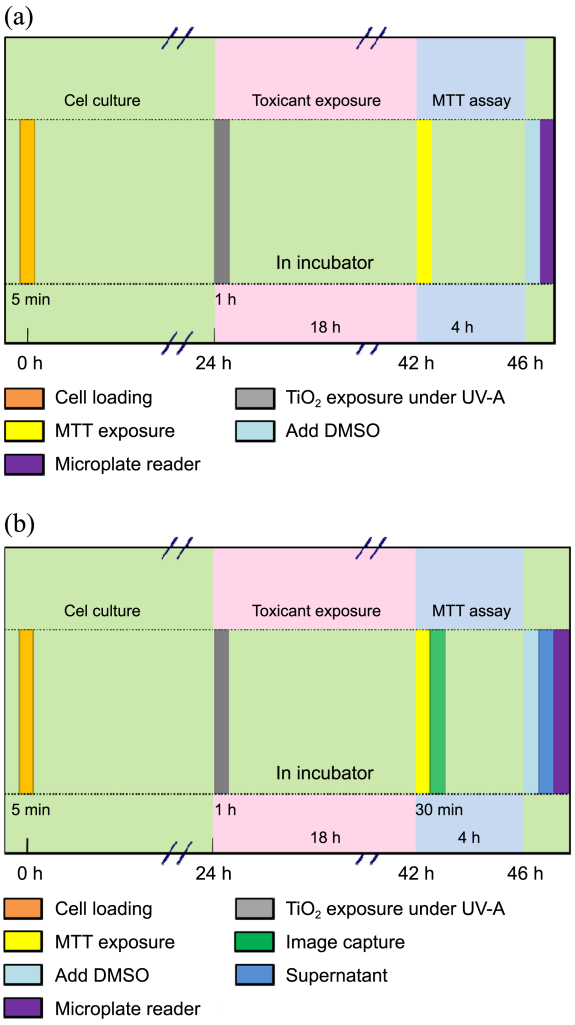

Figure 1. Schematic diagrams of MTT assay protocols with (a) conventional and (b) alternative method.

Cell Culture and Cytotoxicity Assessment. HeLa cells used in this study were obtained from Korea Biological Resource Center (KBRC) and cultured at 37 °C (5% CO_2) in Dulcecoo's Modified Eagle's medium (DMEM, Gibco, Grand Island, NY, USA) containing 10% FBS and 1% Penicillin-Streptomcyin (Gibco, Grand Island, NY, USA). Conventional MTT test was performed using 96 well microplate reader by using typical MTT protocol displayed in Figure 1(a). Also, image cytometryric MTT test was performed and analyzed by using new protocol displayed in Figure 1(b).

Bright-field Optical Image Acquisition. To perform image cytometric MTT assay, bright-field optical images were acquired for each sample using inverted type fluorescence microscope (Olympus IX51, Japan) equipped with cooled CCD camera (QICAM 12-bit Mono Fast 1394, QImaging Ltd., Canada) and appropriate optical filter set (FITC-A-Basic, Semrock, Rochester, NY, USA). The optical filter set, having a peak centered at 530 nm with a spectral bandwidth of 43 nm, was chosen to provide a monochromatic light necessary for obtaining MTT-formazan absorbance images.[13]

Converting Bright-field Image to Absorbance Image. The acquired bright-field optical images were further processed to obtain formazan absorbance images, and then analyzed to obtain cellular information. Since conventional MTT cell viability assay using 96 well plate is based on the measurement of absorbance value of MTT-formazan, bright-field image taken at appropriate wavelength range was transformed into absorbance image in this image cytometry MTT assay protocol. The bright-field optical images were converted to corresponding optical density images by taking minus logarithm of each bright-field image (I_1) divided by a mean value (I_0) of an area on the sample at which no absorption in this wavelength range was observed. As a result, in absorbance image, cells with high content of MTT-formazan appear bright on a dark background and look similar with typical fluorescence image. Additionally, according to the well-known Beer's law, values in absorbance image are proportional to the concentration of absorbing compounds (*e.g.*, MTT-formazan).[13]

Image Cytometry Analysis. The morphological and MTT-formazan absorbance information for each cell (*e.g.*, cell circularity, cell area, mean/integrated absorbance of individual cells) were extracted by using java-based image processing and analysis software (ImageJ 1.41n, NIH, USA). For automated processing of numerous images obtained from each sample, ImageJ macro, involving 1) cell segmentation, 2) bright-field to absorbance image transformation, 3) cellular

information measurement functions, were made and applied to extract cellular information from each optical image. Segmentation of cellular area was performed on the bright-field image to obtain ROI (region of interest) and each bright-field image was transformed to absorbance image, then the ROIs were applied to absorbance image to extract cellular absorbance information (*e.g.*, mean and integrated cellular absorbance) of each cell.[13]

Results and Discussion

In Figure 2, a bar graph of the optical densities at 595 nm (OD595), photographs and the UV/Vis absorption spectra of an MTT assay results performed under UV-A exposure conditions in the absence of HeLa cells are presented. These results clearly demonstrate that the presence of TiO_2 NPs in the cell culture media could results in abiotic reduction of MTT to formazan. As shown in Figure 2(a), the presence of TiO_2^{P25} or DMEM exposed to UV-A significantly increased the OD595 (approximately 2-fold enhancement), even in the absence of HeLa cells. Moreover, adding TiO_2^{P25} NPs to DMEM media have resulted in 6-fold enhancement in the OD595 values measured by the microplate reader. The photographs and absorption spectra shown in Figure 2(b) and 2(c) further confirmed sources of errors during nano-toxicity assays using conventional MTT protocol. The enhancements in OD baselines for samples '1' and '5' (TiO_2^{P25} in PBS and DMEM, respectively) suggested that the light scattering by aggregated/agglomerated TiO_2^{P25} NPs contributes significantly to the OD595. The broad absorption peaks in samples '3'-'6' (DMEM with and without TiO_2^{P25} NPs) in the 500-600 nm (570 nm) range confirms the abiotic reduction of MTT to formazan under these conditions.

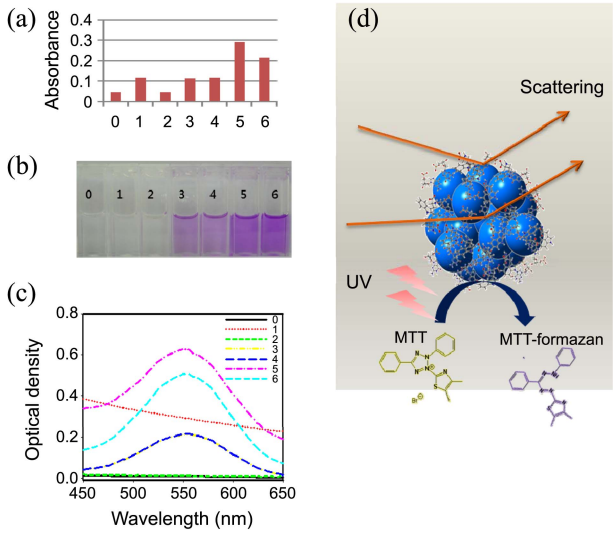

Figure 2. (a) A bar graph of optical densities at 595 nm (OD595) collected from a 96-well plate reader. (b) photographs and (c) UV-Vis absorption spectra of an MTT assay results performed under UV-A exposure conditions, but in the absence of HeLa cells. Sample numbers in (b) and (c) indicate the following conditions; '0' (PBS only), '1' (TiO_2^{P25} in PBS), '2' (supernatant of sample '1' after centrifugation), '3' (DMEM only), '4' (supernatant of sample '3' after centrifugation), '5' (TiO_2^{P25} in DMEM), '6' (supernatant of sample '5' after centrifugation). (d) Schematic diagram of two main sources of error when using conventional MTT assay to assess NPs toxicity.

These observations imply that there are at least two main sources of error when using the conventional MTT assay to assess NPs toxicity: 1) light scattering by aggregated/agglomerated NPs and 2) photocatalytic MTT reduction to formazan in DMEM with or without TiO_2^{P25} NPs (see Figure 2D). The DMEM components seem to play an important role in photocatalytic MTT reduction, but it becomes much more enhanced in the presence of TiO_2^{P25} NPs. Consequently, these errors may cause significant overestimations in MTT-based viability measurements. Similar artifacts have been attributed to the optical properties of NPs (*e.g.*, absorption and light scattering) and extracellular abiotic interactions between MTT or formazan and NPs (*e.g.*, reduction, adsorption, or both).[2,10]

Artifacts caused by light scattering and photocatalytic reduction were also confirmed by comparing conventional MTT assay results of TiO_2^{P25} for the HeLa cell line. A conventional MTT cell viability assay was used to compare TiO_2^{P25} (bulk TiO_2^{P25}) and $TiO_2^{P25\text{-}70}$ (the TiO_2^{P25} fraction less than 100 nm in mean hydrodynamic size)[11] (see Figure 3(a)

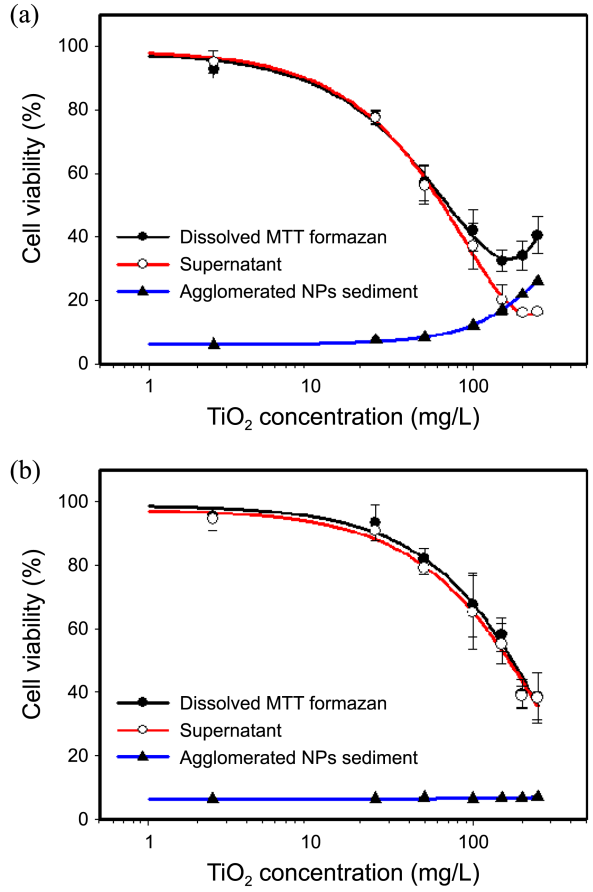

Figure 3. Comparison of conventional MTT assay results of (a) TiO_2^{P25} and (b) $TiO_2^{P25\text{-}70}$ (cell viability measured for the whole suspensions, supernatants and sediments were denoted as filled circles, hollow circles and filled triangles, respectively).

and 3(b)). TiO_2 NPs scattered light in a size- and dose-dependent manner. As shown in Figure 3(a), aggregated/agglomerated NPs in the high TiO_2^{P25} dose significantly contributed to light scattering in an MTT cell viability assay. The results of bulk TiO_2^{P25} suspensions (Figure 3(a), filled circles) display a typical viability trend at low to intermediate concentrations (< 100 mg/L), but with an unusual increase in cell viability at high TiO_2 concentrations (> 100 mg/L). To clarify reasons for this unusual enhancement in cell viability, supernatants and sediments of the whole suspensions were assayed independently and presented as an overlay plot (see Figure 3(a), hollow circles and filled triangles). This plot confirms that the unusual rise in cell viability at high TiO_2 concentrations is mainly due to highly aggregated/agglomerated TiO_2^{P25} nanoparticles. On the other hand, as shown in Figure 3(b), MTT assays of both whole suspension and the supernatant of TiO_2^{P25-70} were found almost identical (hollow and filled circles, respectively). It is evident that the light scattering by TiO_2^{P25} particles results in a significant overestimation of MTT-based cell viability when high NPs doses were applied and/or strong aggregation/agglomeration occur during the measurement. Therefore, this artifact should be carefully considered and minimized during nanotoxicity assessments, especially when the sample contains large fractions of highly aggregated/agglomerated particles. However, this artifact from light scattering can be circumvented with slight modifications of the current assay protocol, such as including centrifugation step or collecting the supernatant before measuring the OD values.

However, in addition to this optical interference due to the light scattered by aggregated/agglomerated NPs, there is a more important artifact, such as the photocatalytic reduction of MTT to formazan by the TiO_2 NPs. For example, the dose-response curves in Figure 3(b) might still include artifacts caused by abiotic MTT reduction by TiO_2 NPs. To minimize this artifact from abiotic MTT reduction, it is necessary to exclude signals from extracellularly (*i.e.*, abiotically) reduced formazan precipitates. Recently, we have reported an image cytometric MTT assay protocol and reported its performance in assessing viability of cells exposed to Cd^{2+} ions within microfluidic device.[13] By adapting above image cytometry MTT assay protocol for the cytotoxicity assessment of TiO_2 NPs, only the intracellularly reduced formazan absorbance can be measured.[13,14] The bright-field images and scatter plot shown in Figure 4(a) demonstrate the ability of image cytometry MTT assay protocol to minimize the artifacts caused by extracellular MTT reduction. As shown in the inset of Figure 4(a), bright-field images of control cells contained highly absorbing cells with clean backgrounds, while cells exposed to 250 mg/L TiO_2^{P25-70} displayed weakly absorbing cells with many formazan-TiO_2 precipitates, appearing as tiny spots in the inset images. These differences were further confirmed in the scatter plot shown in Figure 4(a) (integrated absorbance *vs*. area), where smaller spots of extracellular formazan associated with or without TiO_2 NPs were clearly distinguished from much larger cells containing formazan precipitates.

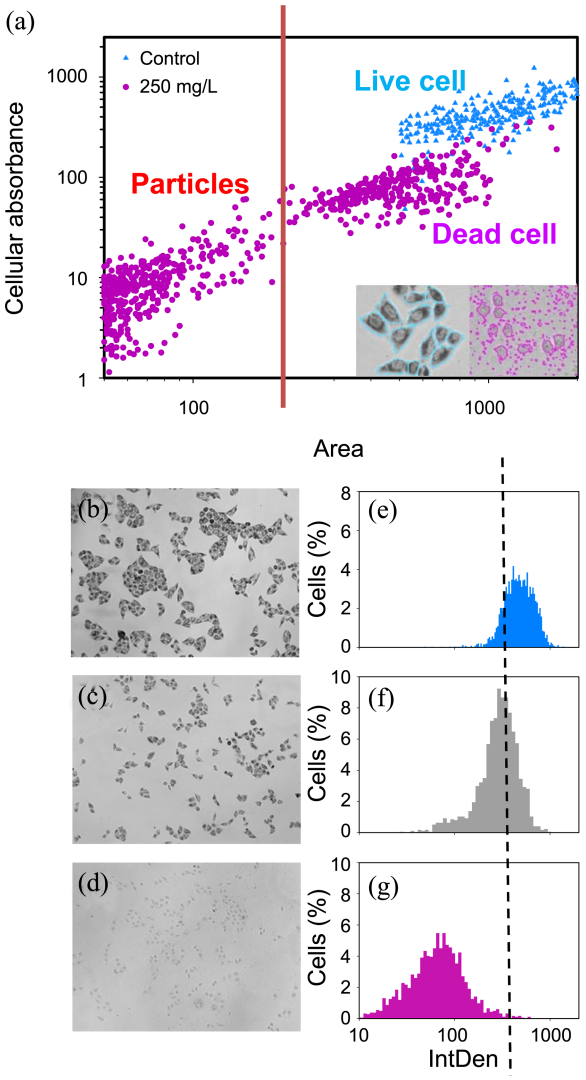

Figure 4. (a) Scatter plots of image cytometric analysis results. Filled triangles and circles represent distributions obtained from control HeLa cells and those exposed to 250 mg/L TiO_2^{P25-70}, respectively. Bright-field optical images (b)-(d) and histograms of cellular absorbance (e)-(g) of HeLa cells exposed to TiO_2^{P25-70} NPs. (b) and (e) correspond to control, (c) and (f) correspond to HeLa cells exposed to 100 mg/L TiO_2^{P25-70} NPs, and (d) and (g) correspond to HeLa cells exposed to 250 mg/L TiO_2^{P25-70} NPs.

Live and dying/dead cells were mostly found in the top- and middle- right regions of the scatter plot (area: > 200, integrated absorbance > 30), while extracellular formazan-TiO_2 precipitates were found in the lower left corner of the scatter plot (area: < 200, integrated absorbance < 30). Thus, by applying a minimum cutoff size (area > 200) for the objects in this scatter plot, we can easily distinguish extracellularly formed formazan precipitates from live and dying/dead cells with intracellularly formed MTT-formazan.

Figure 4(b-g) shows bright-field images (b-d) and the distributions of cellular formazan absorbance (e-g) obtained from image cytometry of HeLa cells exposed to three different TiO_2^{P25-70} levels ([TiO_2] = 0 mg/L, 100 mg/L, and 250 mg/L). The control cells (unexposed to TiO_2) had a

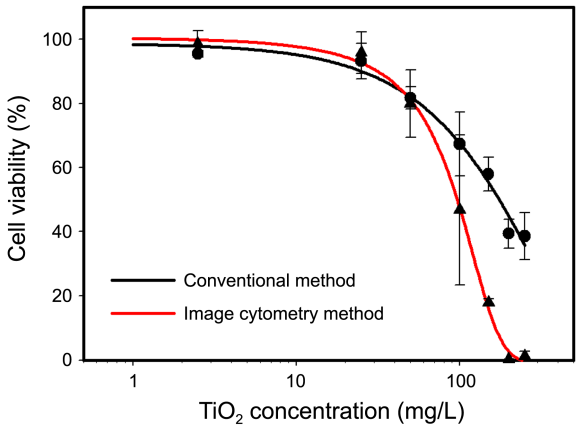

Figure 5. Comparison of dose-response curves obtained from conventional MTT cell viability assay (filled circles) and image cytometry based MTT assay (filled triangles) performed for HeLa cells exposed to the $TiO_2^{P25\text{-}70}$ suspensions. Minimum cut-off size (area > 200) for objects in this scatter plot, we can easily distinguish extracellular formazan precipitates from live and dying/dead cells with intracellularly formed MTT-formazan.

mean cellular absorbance of 447 ± 113, while those cells exposed to high $TiO_2^{P25\text{-}70}$ levels (250 mg/L) had much lower cellular absorbance (67 ± 31). These observations agreed well with our expectation that healthy adherent cells will have a relatively high formazan absorbance due to the high mitochondrial enzyme activity (MEA) of living cells, while cells exposed to high NPs concentrations will have greatly reduced absorbance due to cell death and the subsequent decrease in MEA. The vertical line in the histogram (at a cellular absorbance of 333) indicates the boundary between MEA(+) and MEA(−), which corresponds to the position of 1σ less than the mean cellular absorbance of control cells.

The same image cytometry analysis procedure was applied for all exposure conditions, and the image cytometry based dose-response curve is compared with the conventional approach in Figure 5. This comparison demonstrates that, at high dose of $TiO_2^{P25\text{-}70}$ NPs ($[TiO_2]$ > 50 mg/L), the cell viability from image cytometry approach is significantly lower than those viability values measured from the conventional MTT assay (see Figure 5, filled circles and triangles for conventional and image cytometry based MTT cell viability results, respectively). Since it was previously confirmed that scattered light have negligible contribution for this suspensions of $TiO_2^{P25\text{-}70}$ NPs under these conditions, the observed difference in Figure 5 can be mostly attributed to extracellular abiotic MTT reduction. As the $TiO_2^{P25\text{-}70}$ concentration increases, it seems that the photocatalytic MTT reduction at the TiO_2-water interface become more significant and resulted in larger differences at higher doses. The LC50 of $TiO_2^{P25\text{-}70}$ estimated from conventional MTT assay is about 160 mg/L, while the image cytometry MTT assay resulted in an LC50 of 96 mg/L. These results suggest that the conventional MTT assay overestimates LC50 by 40% (*i.e.*, 64 mg/L), due to photocatalytic MTT reduction in the presence of TiO_2 and DMEM.

Despite increasing importance of *in vitro* cell-based assays for the assessment of nanotoxicity, their suitability for the nanotoxicity assessment is still in doubt. In this study, current limitations of widely used MTT cell viability assay protocol were carefully examined for the cytotoxicity assessment of P25 TiO_2 NPs and an alternative toxicity assessment protocol based on image cytometry approach was developed to overcome these limitations. We have found two important artifacts in conducting conventional MTT cell viability assay for the P25 TiO_2 NPs, which are 1) light scattering by aggregated/agglomerated NPs and 2) abiotic and photocatalytic reduction of MTT to formazan in the presence of DMEM and/or TiO_2^{P25} NPs. Abiotic and photocatalytic MTT reduction can be overcome by applying image cytometry approach to measure only the intracellular formazan while excluding extracellularly formed formazan, while the artifact induced by the scattered light can be minimized by slight modifications of the current assay protocol, such as adding centrifugation step or collecting the supernatant before measuring the OD values.

Alternative assay protocols that can reliably and accurately assess cytotoxicity of NPs will have a crucial role for the unbiased assessments of NPs cytotoxicity and also have utmost importance in providing solid scientific basis for future regulation of manufactured nanomaterials. Recently, Working Party on Manufactured Nanomaterials (WPMN) of Organization for Economic Co-operation and Development (OECD) have emphasized importance of developing alternative testing methods needed to assess nanotoxicity by recommending prioritized co-operation on this issue.[15] Compared to the conventional cell based assays measuring cellular responses collectively, the cytometric approach measuring individual cellular information seems to have huge potential as an alternative assay protocols that can circumvent or overcome various limitations of nanotoxicity assessments. For instance, recent flow cytometry studies by Zucker *et al.*[16] have provided useful insight into the detection of cellular NP associations and resultant toxicities, while Suzuki *et al.*[17] have proposed scattering-based flow cytometry as a simple and easy method to evaluate cellular association of NPs that can be used as a cost-effective technique for initial screening of the nanotoxicity. Thus, we believe that the image cytometry based MTT cell viability assay protocols proposed in this study also provided a simple, reliable, and unbiased method to evaluate nanotoxicity of TiO_2 NPs and can be further modified and expanded for the cytotoxicity assessment of various manufactured nanomaterials.

Conclusion

In this study, we have confirmed that the image cytometry MTT assay can help overcome limitations of the conventional MTT viability assay by selectively measuring intracellular formazan. Moreover, we also believe that the image cytometry MTT assay protocols can further expands its applications for the cytotoxicity assessment of various manufactured nanomaterials, which often cause problems with conventional assay protocols.[5,7]

Acknowledgments. This work was supported by the Korean Ministry of Environment and the Eco-Technopia 21 Project (091-091-081).

References

1. Nel, A.; Xia, T.; Madler, L.; Li, N. *Science* **2006**, *311*, 622.
2. Oberdorster, G.; Oberdorster, E.; Oberdorster, J. *Environ. Health Perspect.* **2005**, *113*, 823.
3. Kroll, A.; Pillukat, M. H.; Hahn, D. *Eur. J. Pharm. Biopharm.* **2009**, *72*, 370.
4. Marquis, B. J.; Love, S. A.; Braun, K. L.; Haynes, C. L. *Analyst* **2009**, *134*, 425.
5. Laaksonen, T.; Santos, H.; Vihola, H.; Salonen, J.; Riikonen, J.; Heikkila, T.; Peltonen, L.; Kumar, N.; Murzin, D. Y.; Lehto, V. P.; Hirvonen, J. *Chem. Res. Toxicol.* **2007**, *20*, 1913.
6. Belyanskaya, L.; Manser, P.; Spohn, P.; Bruinink, A.; Wick, P. *Carbon* **2007**, *45*, 2643.
7. Worle-Knirsch, J. M.; Pulskamp, K.; Krug, H. F. *Nano Lett.* **2006**, *6*, 1261.
8. Casey, A.; Davorne, M.; Herzog, E.; Lyng, F. M.; Byrne, H. J.; Chambers, G. *Carbon* **2007**, *45*, 34.
9. Pfaller, T.; Puntes, V.; Casals, E.; Duschl, A.; Oostingh, G. J. *Nanotoxicology* **2009**, *3*, 46.
10. Wittmaack, K. *Environ. Health Perspect.* **2007**, *115*, 187.
11. Kwon, D.; Lee, S. H.; Kim, J.; Yoon, T. H. *Toxicol. Environ. Health Sci.* **2010**, *2*, 78.
12. Lee, S. H.; Kwon, D.; Yoon, T. H. *Toxicol. Environ. Health Sci.* **2010**, *2*, 207.
13. Lim, K. H.; Park, J.; Rhee, S. W.; Yoon, T. H. *Cytom. Part A* **2012**, *81A*, 691.
14. Kim, M. J.; Lim, K. H.; Yoo, H. J.; Rhee, S. W.; Yoon, T. H. *Lab. Chip*. **2010**, *10*, 415.
15. Draft recommendation of the council on the safety testing and assessment of manufactured nanomaterials. 11th meeting of the working party on manufactured nanomaterials. 19-21 Fevruary 2013, OECD conference centre 2 rue André-Pascal, Paris, France.
16. Zucker, R. M.; Massaro, E. J.; Sanders, K. M.; Degn, L. L.; Boyes, W. K. *Cytom. Part A* **2010**, *77A*, 677.
17. Suzuki, H.; Toyooka, T.; Ibuki, Y. *Environ. Sci. Technol.* **2007**, *41*, 3018.